Journal of Biomechanics 46 (2013) 1098–1103

Contents lists available at SciVerse ScienceDirect

Journal of Biomechanics

journal homepage: www.elsevier.com/locate/jbiomech
www.JBiomech.com

Precision grip responses to unexpected rotational perturbations scale with axis of rotation

Michael De Gregorio, Veronica J. Santos *

Mechanical and Aerospace Engineering, Arizona State University, Tempe, AZ, USA

ARTICLE INFO

Article history:
Accepted 13 January 2013

Keywords:
Catch-up response
Fingertip forces
Rotational slip
Torque loads
Unexpected loads

ABSTRACT

It has been established that rapid, pulse-like increases in precision grip forces ("catch-up responses") are elicited by unexpected translational perturbations and that response latency and strength scale according to the direction of linear slip relative to the hand as well as gravity. To determine if catch-up responses are elicited by unexpected rotational perturbations and are strength-, axis-, and/or direction-dependent, we imposed step torque loads about each of two axes which were defined relative to the subject's hand: the distal–proximal axis away from and towards the subject's palm, and the grip axis which connects the two fingertips. Precision grip responses were dominated initially by passive mechanics and then by active, unimodal catch-up responses. First dorsal interosseous activity, marking the start of the catch-up response, began 71–89 ms after the onset of perturbation. The onset latency, shape, and duration (217–231 ms) of the catch-up response were not affected by the axis, direction, or magnitude of the rotational perturbation, while strength was scaled by axis of rotation and slip conditions. Rotations about the grip axis that tilted the object away from the palm and induced rotational slip elicited stronger catch-up responses than rotations about the distal–proximal axis that twisted the object between the digits. To our knowledge, this study is the first to investigate grip responses to unexpected torque loads and to show characteristic, yet axis-dependent, catch-up responses for conditions other than pure linear slip.

1. Introduction

When objects in precision grip were perturbed by unpredictable pulling loads, a rapid initial increase in grip force rate, in the form of a "pulse-like" catch-up response (Johansson et al., 1992c), allowed the delayed reactive grip force to catch up to the unexpected load force and maintain a safety margin against linear slip (Johansson and Westling, 1988). Features of the catch-up response such as onset latency, shape, and duration were independent of load force amplitude (Johansson et al., 1992c) and frictional condition (Cole and Johansson, 1993). When load force rate increased, strength of the catch-up response increased and onset latency decreased while duration of the catch-up response remained 200 ms (Johansson et al., 1992b). The stereotypical features of the catch-up response suggested it was a centrally-programmed, default grip response that was released as a unit in response to unexpected loading (Johansson et al., 1992a, 1992b, 1992c). These findings supported observations of evoked, automatic reactive grip responses (Cole and Abbs, 1988).

Studies involving self-imposed rotational perturbations suggested that slip conditions may scale grip responses. While linear slip is caused by forces tangential to the grip surface, rotational slip is caused by torques about the axis perpendicular to the grip surface (Kinoshita et al., 1997). However, prior experiments on rotational slip used voluntary tasks such as lifting and holding (Jenmalm et al., 2000), lifting and tilting (Goodwin et al., 1998), or releasing one's grasp to allow tilting (Kinoshita et al., 1997). These studies focused only on torque loads about the "grip axis" which connects the two fingertips.

The objectives of this study were twofold: to determine if a catch-up response is elicited by *unexpected rotational perturbations*, and, if so, to determine if features of the catch-up response (onset latency, shape, duration, strength) are dependent on the direction, strength, and/or axis of the perturbation. To our knowledge, this is the first study to investigate grip responses to unexpected torque loads and to show characteristic, yet axis-dependent, catch-up responses for conditions other than pure linear slip.

2. Materials and methods

2.1. Experiment

Eighteen consenting, healthy, right-handed subjects aged 19–38 years (nine male, nine female) participated in the study under a protocol approved by the Arizona State University Institutional Review Board.

* Correspondence to: Mechanical and Aerospace Engineering, Arizona State University, 501 E. Tyler Mall, ECG 301, MC 6106, Tempe, AZ 85287-6106, USA. Tel.: +1 480 965 3207; fax: +1 480 727 9321.
E-mail address: veronica.santos@asu.edu (V.J. Santos).

0021-9290/$ - see front matter © 2013 Elsevier Ltd. All rights reserved.
http://dx.doi.org/10.1016/j.jbiomech.2013.01.017

A motion-capture system (MX-T40 cameras, Vicon) and 3 mm diameter hemispherical markers (Mocap Solutions) were used to collect kinematic data at 200 Hz from the thumb and index finger of each subject's dominant hand and an instrumented object (Fig. 1A). Surface electromyography (EMG) was used to measure the activity of the first dorsal interosseous (FDI) muscle (EMG 100C, BIOPAC Systems).

The instrumented object had two flat, parallel grip surfaces spaced 39 mm apart. Fingertip forces and torques were measured independently for the thumb and index finger at 1.8 kHz by six degree-of-freedom force/torque transducers (Nano-25, ATI Industrial Automation) housed within the object, whose total mass was 194 g with the transducers. The aluminum grip plates were covered by a single layer of masking tape in order to minimize reflectivity during motion capture.

Rotational perturbations were imposed about two axes which were defined relative to the subject's hand, fixed relative to the object, and passed through the object's center of mass (Fig. 1A): the distal–proximal ("*d–p*") axis away from and towards the subject's palm, and the grip axis. Positive and negative rotations were imposed about the *d–p* axis while only a negative rotation was imposed about the grip axis such that the top of the object tilted away from the subject's palm. Perturbations were imposed using a mass and pulley system attached to the object via lightweight, inextensible fishing line (200 lbf braided line, PowerPro). An unexpected, step torque load was imposed during each 5 s trial by dropping a mass (100 g or 150 g) vertically by 5 cm at a random time and leaving the mass hanging. No significant swinging of the mass was observed. *Object-moments* (externally-applied torque loads) were imposed by attaching the fishing line to points 34.3 mm above or below the object's center of mass (Fig. 1B, Table 1).

Each subject sat upright with the dominant arm supported by a tabletop, elbow flexed, and forearm parallel to the tabletop and perpendicular to the subject's frontal plane. With each subject's dominant hand and wrist unsupported at the end of the table, a vacuum positioning pillow (Versa Form, Sammons Preston) and velcro strap constrained the subject's forearm to the tabletop. Hand pronation and supination were restricted while wrist flexion/extension and radio-ulnar deviation were not.

At the start of each 5-trial experimental block, subjects were handed the instrumented object and instructed to hold the object upright using a precision grip with the thumb and index finger each centered on its own grip plate and directly opposed to one another, with the other digits curled towards their palm as if making a fist (Fig. 1A). The instructions given to subjects were to hold the object with just enough force to keep it aloft, return the object to its initial orientation as soon as a randomly-timed perturbation was detected, avoid dropping the object, and notify the researcher if he/she felt fatigued. To minimize visual cues about the perturbation, subjects were instructed to look towards a fixed location away from the object and investigator. There were no auditory cues for the perturbation.

Presented to subjects in the order shown in Table 1, six experimental blocks used combinations of levels for three factors: axis of rotation (*d–p*, grip axis), direction of rotation (positive, negative), and object-moment magnitude (small, large). After each block, subjects received a mandatory 30 s rest period during which the object was taken from the subject and prepared for the next block. No practice trials were allowed.

Table 1
Experimental block conditions. Each experimental block consisted of five trials followed by a mandatory rest period and were presented to each subject in the order shown. The experimental factors investigated were axis of rotation, direction of rotation, and object-moment magnitude.

Experimental block #	Experimental factors		
	Axis of rotation	Direction of rotation	Object-moment magnitude (OMM) (mN m)
1	Distal–proximal	Positive	33.6
2			50.5
3		Negative	50.5
4			33.6
5	Grip	Negative	33.6
6			50.5

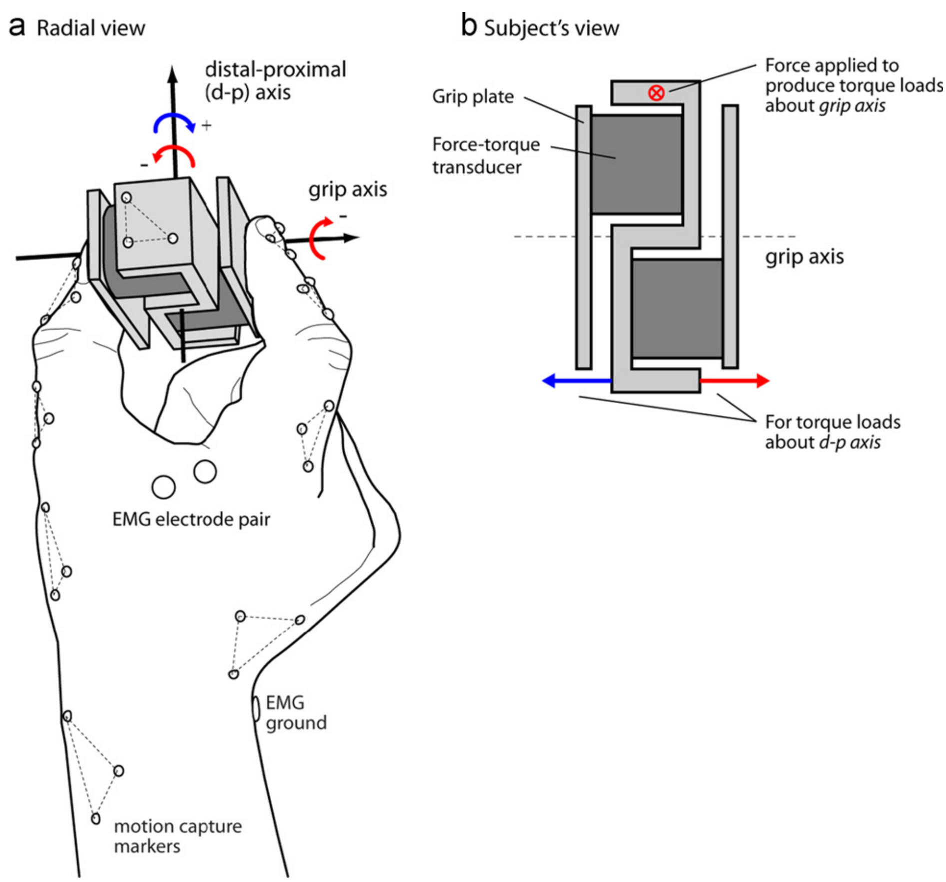

Fig. 1. Experimental set-up. (A) A radial view of the subject's hand is shown with triads of retro-reflective markers (indicated by dotted lines) that were used to track the motion of the thumb, index finger, and instrumented test object. Surface EMG was used to record first dorsal interosseous activity. Directions of rotation (red = negative, blue = positive) are defined as shown with respect to each of two hand-referenced, object-fixed axes: distal–proximal and grip axes. (B) A view from the perspective of the subject of the object shows the locations of the attachment points used to impose rotational perturbations with a cable, mass, and pulley system. (For interpretation of the references to color in this figure legend, the reader is referred to the web version of this article.)

2.2. Data analysis

Motion capture data were processed with MATLAB (Mathworks) after using Vicon Nexus software to ensure complete marker sets. Object kinematics were used to determine the onset of object perturbation (defined as "$t=0$ s"), verify the predominance of rotational motion in each perturbation, and synchronize trials. Angular deviations of the object from its initial upright orientation were measured about the axis of interest (Fig. 1A) and averaged across trials for each block on a subject-specific basis. Extracted from mean data, the peak angular deviation of the object was defined as the maximum magnitude of rotation of the object from its initial orientation.

FDI surface EMG data were full-wave rectified, filtered using a fourth-order, 50 Hz low-pass Chebyshev filter (Hodges and Bui, 1996), and normalized using maximum voluntary contraction data collected at the start of the experiment. For each subject, all trials for a given block were averaged to ensure that trends in muscle activation were consistent. Conservative activation threshold values were set at three standard deviations of the baseline noise prior to the onset of object perturbation (averaged over each subject-specific block). The FDI was deemed active if EMG activity (averaged over a single block) remained above threshold for a continuous period of at least 50 ms (Hodges and Bui, 1996). Visual inspection verified that the activation thresholds resulted in reliable threshold crossings (Di Fabio, 1987). The time to initial FDI activation (time of the first upward threshold crossing relative to the onset of object perturbation) was used as the *onset latency of the catch-up response*. Due to poor connectivity, EMG data is only presented for 15–17 subjects, depending on the perturbation conditions.

Fingertip force and torque data were filtered using a fourth order, 30 Hz low-pass Butterworth filter (Jordan and Newell, 2004). Force data for individual trials were averaged for each block on a subject-specific basis to ensure consistent extraction of key features (Edin et al., 1992; Cole and Johansson, 1993; Goodwin et al., 1998; Jenmalm et al., 2000). Normal force rates were obtained from first-order differences of normal forces for each individual trial while accounting for sampling rate, averaging those data for each block on a subject-specific basis, and smoothing with a moving boxcar average having a width of 50 ms. Extracted from mean data, peak normal force was used to mark the end of the catch-up response in order to determine the duration of the catch-up response, and peak normal force rate was used to define the *strength of the catch-up response*.

2.3. Statistical analysis

The data could not be transformed into normal distributions using square-root, log, or inverse sine functions. Thus, we used the Kruskal–Wallis test (nonparametric analog to the one-way ANOVA) with an alpha level of 0.05 to evaluate the independent effects of three factors: axis of rotation (*d–p*, grip), direction of rotation (positive, negative), and object-moment magnitude (small, large) (Table 1), and to test whether quantities of interest could be pooled across digits. Summary data are reported as either median ranges or median ± median absolute deviation (MAD) unless otherwise specified.

3. Results

For rotations about the *d–p* axis, the object was twisted clockwise or counter-clockwise as viewed from the subject's perspective (Fig. 1). For rotations about the grip axis, the top of the object was tilted away from the subject's palm. Subjects could halt the tilting, but were unable to restore the object to its initial upright orientation.

Shortly after the onset of perturbation, FDI became active and a unimodal catch-up response began (Fig. 2), during which digit normal forces increased and decreased in parallel. The period from the onset of perturbation ("a", Fig. 2) until FDI activation ("b", Fig. 2) was considered as the passive phase, and was characterized by smooth, unimodal tangential fingertip forces immediately after the onset of perturbation (Fig. 3). The large ± MAD ranges after FDI activation were consistent with an increase in neuromuscular activity.

An active unimodal catch-up response was clearly observed in the normal force rates for all subjects, both digits, and all blocks (representative block shown in Fig. 2, multiple blocks shown in Fig. 5). The catch-up response began with FDI activation ("b", Fig. 2) and ended with peak normal force ("d", Fig. 2). FDI activity began 71–89 ms after the onset of perturbation (Fig. 4, Table 2), the time to peak normal force was 283–319 ms after the onset of perturbation, and the duration of the catch-up response was 217–231 ms (Table 2). Time to peak normal force rate (127–152 ms, Table 2), onset latency, and duration of the catch-up response were not affected by any experimental factor: axis of rotation, direction of rotation, or object-moment magnitude.

For all subjects, digits, and object-moment magnitudes, the strength of the catch-up response and peak normal force were greatest for rotational perturbations about the grip axis (Figs. 5 and 6, Table 2), which tilted the top of the object away from the subject's palm and induced rotational slip. Strength of the catch-up response and peak normal force were 31–55 N/s and

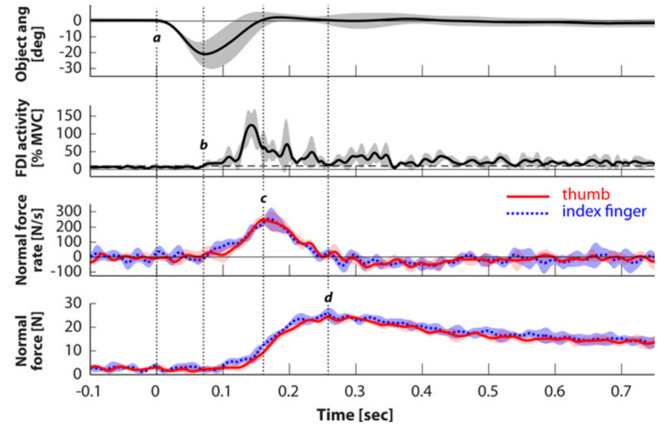

Fig. 2. Object angle, FDI activity, normal force rate, and normal force as a function of time. Mean data are reported for a representative subject for a single block of experiments (large object-moment magnitude, negative rotation about the distal–proximal axis) for angle of deviation of the object, FDI activity (normalized by maximum voluntary contraction (MVC)), normal force rate, and normal force. The index finger (mean=dotted blue line) and thumb data (mean=solid red line) could be pooled. The shaded region (blue and red for index finger and thumb, respectively) around each mean trace represents ± SEM across five trials. Vertical dotted lines indicate times for: a onset of perturbation; b start of the catch-up response (time to FDI activation); c peak normal force rate (strength of catch-up response); and d end of the catch-up response (peak normal force). A distinct unimodal catch-up response was observed in the normal force rate data for each digit. (For interpretation of the references to color in this figure legend, the reader is referred to the web version of this article.)

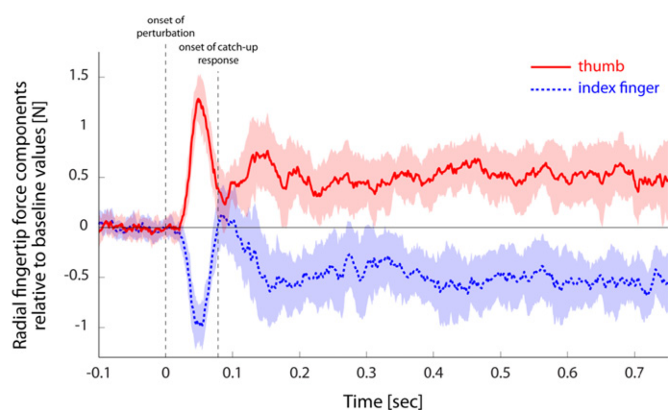

Fig. 3. Variability in radial fingertip force components. For clarity, radial force components relative to baseline values (prior to perturbation) are shown in order to account for trial-to-trial variations in baseline fingertip forces. Trends are shown for negative rotations about the distal–proximal axis, for all 18 subjects, for both object-moment magnitudes ($n=35$ trials total), and both the thumb (solid red line) and index finger (dotted blue line). Thick lines represent median values and shaded regions represent the ± MAD ranges. Radial force components exhibited the least variability from the onset of perturbation (dashed vertical line at $t=0$ s) to first dorsal interosseous activation at 83.9 ± 12.8 ms (dashed vertical line marking the onset of catch-up response). (For interpretation of the references to color in this figure legend, the reader is referred to the web version of this article.)

6–7 N greater for rotations about the grip axis than for rotations about the *d–p* axis, respectively. Strength of the catch-up response was not affected by direction of rotation and was only affected by object-moment magnitude for one type of rotation (positive rotations about the *d–p* axis, Fig. 6).

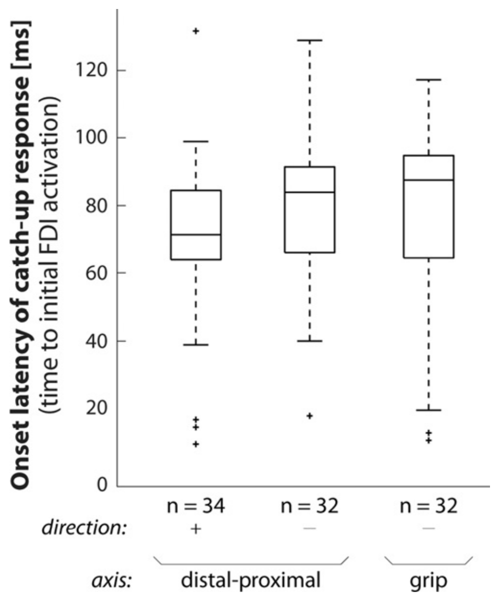

Fig. 4. Onset latency of the catch-up response (time to first dorsal interosseous activation). The box plots show the time to first dorsal interosseous (FDI) activation which was used to mark the start of the catch-up response. FDI was considered to be active if the surface EMG signal crossed a threshold of 3 SD of the baseline noise and remained above threshold for at least 50 ms. Short latency values resulted from the fact that we report time to *first* activation according to our conservative activation criteria even though FDI activity may have briefly fallen below the activation threshold afterwards. Each box plot consists of data pooled across the small and large object-moment magnitudes for each rotation condition (from left to right: n=[34, 32, 32] mean values total). Each box plot indicates the 25th, 50th, and 75th percentiles. The whiskers indicate the 10th and 90th percentiles. Outliers (indicated by "+") had values that were more than 1.5 times the interquartile range from the top or the bottom of the box.

4. Discussion

4.1. Existence of the catch-up response for rotational perturbations

Prior studies described the catch-up response as a means by which subjects maintained a stable grasp when unexpected translational loads were imposed and linear slip was imminent (Johansson et al., 1992b, 1992c; Cole and Johansson, 1993; Häger-Ross and Johansson, 1996; Häger-Ross et al., 1996). We have shown that a characteristic unimodal catch-up response is also elicited in response to unexpected rotational perturbations that induce conditions other than linear slip. The catch-up response was observed for all subjects, both digits, and irrespective of three experimental factors: object-moment magnitude, axis of rotation, and direction of rotation (Fig. 5). Peak normal force and strength of the catch-up response were generally unaffected by torque load or direction of rotation, suggesting that strength of the catch-up response may be similarly robust to torque magnitude as it is to force magnitude (Johansson et al., 1992c).

Due to the perturbation method (Fig. 1B), the external perturbations were not pure rotations but rather combinations of rotation and translation. Nonetheless, a kinematic analysis confirmed that rotational effects were predominant for the (0, 100 ms) period immediately following the perturbation. Future experiments will utilize haptic devices to impose purely rotational perturbations, randomize experimental conditions, and include rotations about a radial–ulnar axis. A direct comparison of intra-subject grip responses to pure rotational slip and pure linear slip is also planned.

4.2. Robust timing of the catch-up response

The temporal characteristics of the catch-up response were robust to experimental conditions. The durations of the catch-up

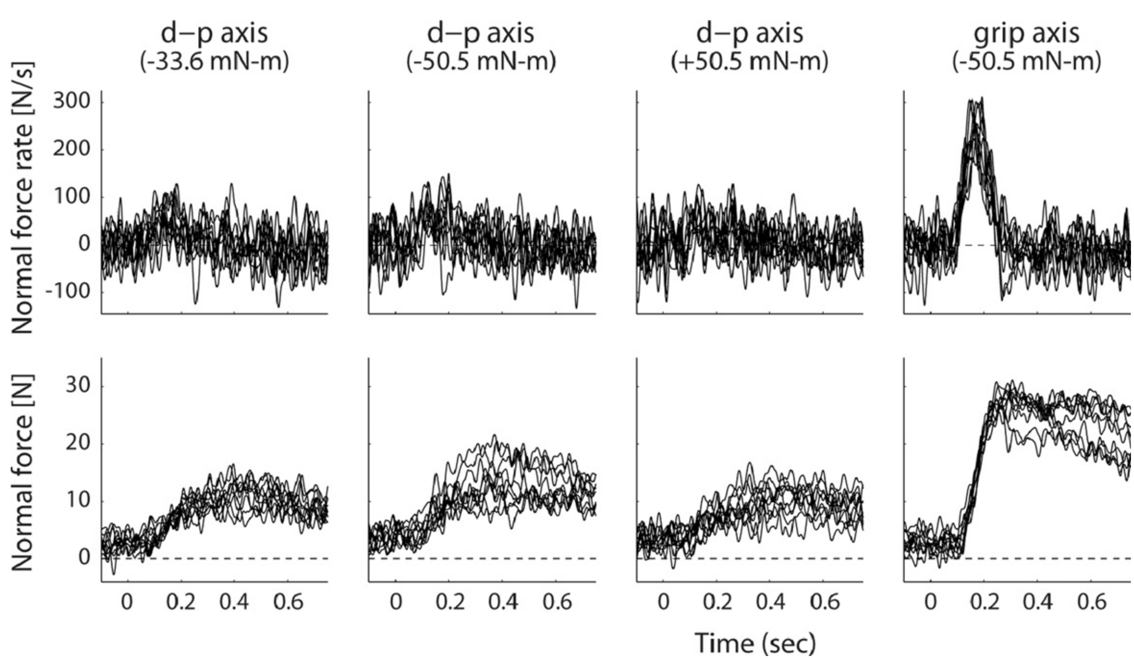

Fig. 5. Normal force rate and normal force as a function of time for different blocks. Unimodal catch-up responses were observed in the normal force rates for all object-moment magnitudes, rotation directions, and rotation axes. Individual trial data (n=5 trials) for one subject are shown here for both digits and five blocks. Catch-up responses were strongest for rotations about the grip axis.

Table 2
Object kinematics and grip response events. Object kinematics and grip response events are summarized for all 18 subjects, pooled across both digits, and pooled by object-moment magnitude (OMM), unless otherwise specified. Data are reported as median ± MAD in the order of key events after the onset of perturbation and are separated according to axis and direction of rotation.

Axis:	**Distal–proximal**		**Grip**
Direction:	**Positive**	**Negative**	**Negative**
Peak angular deviation of object (deg)	Small OMM, 9.5 ± 1.9 Large OMM, 12.7 ± 2.0	Small OMM, 11.7 ± 1.9 Large OMM, 17.8 ± 3.8	Small OMM, 33.6 ± 5.2 Large OMM, 40.5 ± 8.3
Time to peak angular deviation of object (ms)	Small OMM, 55.0 ± 0.0 Large OMM, 65.0 ± 5.0	Small OMM, 60.0 ± 5.0 Large OMM, 70.0 ± 5.0	137.5 ± 25.0
Onset latency of the catch-up response (ms). (*Time to FDI activation, "b" in Fig. 2*)	71.4 ± 9.2	83.9 ± 12.8	88.6 ± 9.2
Strength of the catch-up response (N/s) (Peak normal force rate)	Small OMM, 79.5 ± 21.9 Large OMM, 104.2 ± 27.0	83.4 ± 21.8	134.7 ± 50.8
Time to peak normal force rate (ms) ("c" in Fig. 2)	127.2 ± 15.5	152.2 ± 28.9	145.8 ± 16.7
Peak normal force (N)	13.0 ± 2.9	12.5 ± 3.3	19.2 ± 8.0
Time to peak normal force (ms) ("d" in Fig. 2)	309.2 ± 84.7	319.2 ± 80.5	282.5 ± 45.3
Duration of the catch-up response (ms) (from "b" to "d" in Fig. 2)	230.8 ± 74.7	221.9 ± 79.2	216.9 ± 50.8

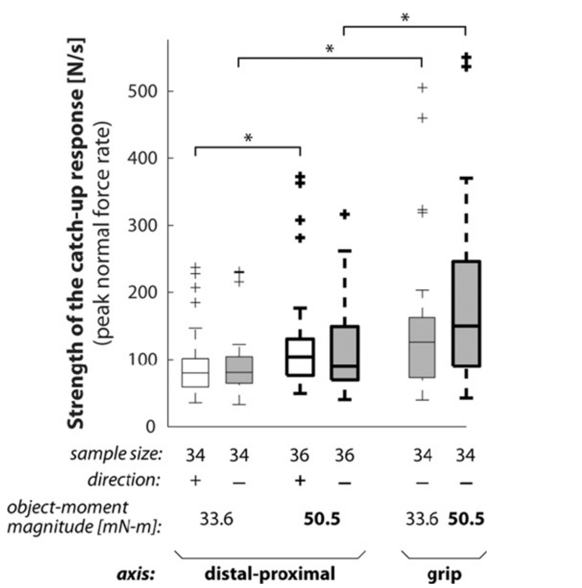

Fig. 6. Strength of the catch-up response (peak normal force rate). Each column represents strength of the catch-up response pooled across the thumb and index finger for 18 subjects. Thicker box plots are used for large object-moment magnitudes. Shaded box plots are used for negative rotations. Catch-up responses were strongest for rotations about the grip axis. Asterisks indicate statistically significantly differences across groups. Each box plot indicates the 25th, 50th, and 75th percentiles. The whiskers indicate the 10th and 90th percentiles. Outliers (indicated by "+") had values that were more than 1.5 times the interquartile range from the top or the bottom of the box.

response (217–231 ms, Table 2) were consistent with previously reported durations of 200–250 ms for unexpected linear slip (Johansson et al., 1992c). Onset latency of the catch-up response (71–89 ms, Fig. 4, Table 2) overlapped with the 50–100 ms range reported for grip force responses to natural slips (Johansson and Westling, 1987) and was not far from the 50–70 ms range reported for the latency of a "phasic burst of muscle activity" after the onset of an unexpected force perturbation (Cole and Abbs, 1988). Prior studies reported catch-up response onset latencies of 80 ± 9 ms (mean ± std) (Johansson et al., 1992c), and 62 ± 9 ms and 74 ± 9 ms for catch-up responses to distal and proximal loads, respectively (Häger-Ross et al., 1996).

The consistent shape and timing of the catch-up response to rotational perturbations across experimental conditions supports the existence of pre-programmed grip responses that ensure early stabilization of the grasped object (Johansson et al., 1992b, 1992c; Wing and Flanagan, 1998). Onset latency was based on FDI activation, but was based on changes in normal force rates in other studies (Johansson et al., 1992c; Häger-Ross et al., 1996). While exact onset threshold criteria for normal force rates were not provided in the literature, the time to FDI activation was essentially coincident with the initial increase in normal force rate (Fig. 2 in this work; Fig. 3 in Johansson et al., 1992c).

4.3. *Axis of rotation affects catch-up response strength*

Axis of rotation relative to the hand had the greatest effect on the catch-up response. Peak normal force and strength of the catch-up response were greatest for rotations about the grip axis (Fig. 5, Table 2). Peak normal forces ranged from 12.5 to 19.2 N (Table 2) and, yet, the time to achieve the peak normal force was consistent (283–319 ms, Table 2). The robust timing suggests that the effects of axis of rotation manifested as changes in strength of the catch-up response.

Changes in the axis of rotation fundamentally changed the loading and slip conditions as well as the contributions of the digits to the passive resistance of the perturbations. With no part of the hand to physically oppose rotations about the grip axis, the rotational slip conditions resulted in the largest peak and time to peak angular deviations, and the strength of the catch-up response may have been scaled up to counter rotational slip, in particular (Fig. 5, Table 2). Rotations about the grip axis are particularly troublesome because of the incompatibility of fingertip force/torque capabilities with the axis of rotation, which passes through both fingertips by definition. Normal grip forces are aligned with the axis of rotation and fingertips cannot actively produce tangential torques in the plane of the fingerpad. The smoothness of tangential forces suggests that passive resistance contributes to at least the first 50 ms of the measured forces (Fig. 3). Along with natural limits on joint motion and skin stretch, viscoelastic fingerpads (Pawluk and Howe, 1999) and passive joint torques (Kuo and Deshpande, 2010) resist perturbations.

The fact that catch-up responses were strongest for rotations about the grip axis (Fig. 5, Table 2) is consistent with prior observations that grip forces are more closely regulated for rotational slip than linear slip (Goodwin et al., 1998; Jenmalm et al., 2000), and that grip responses to unanticipated loads vary with load (and slip) direction, with conservative grip responses being associated with "dangerous [loading] directions," such as away from the palm or in the direction of gravity (Häger-Ross et al., 1996). In particular, stronger grip forces (Jones and Hunter, 1992; Häger-Ross et al., 1996) and shorter grip response latencies (Häger-Ross and Johansson, 1996) were observed in response to force loads away from the palm, although we did not observe axis-dependent effects on grip response latency.

The idea that motion away from the hand constitutes a "dangerous direction" (Häger-Ross et al., 1996) applies to translational perturbations, but is not meaningful for rotational perturbations which lead to simultaneous motion towards and away from the hand. We propose that the grip axis is a "dangerous axis" relative to the *d*–*p* axis, where critical differences exist in the conditions for slip and passive resistance of the digits. Hand posture and orientation of the perturbation with respect to joints may also be factors (Häger-Ross and Johansson, 1996). Rotations about the *d*–*p* axis might be resisted by the stiffnesses of entire digits while rotations about the grip axis might be resisted primarily by fingerpads. Furthermore, subjects were instructed to curl the middle, ring, and little fingers, which likely pre-tensioned the flexor digitorum profundus to resist flexion of the index finger.

The finding that grip responses to unexpected rotational perturbations can be axis-dependent has direct implications on the kinematic and kinetic control of anthropomorphic, high degree-of-freedom artificial hands. We previously showed that rotational perturbations elicited simultaneous ad/abduction and flexion/extension of the thumb carpometacarpal joint (De Gregorio and Santos, 2010). While the "catch-up response" appears to reflect a "grip harder" strategy, the act of gripping "harder" is not necessarily the result of pure flexion for human or artificial hands.

Conflict of interest statement

We confirm that there are no known conflicts of interest associated with this publication and there was no significant financial support for this work that could have influenced its outcome.

Acknowledgments

We thank Kevin Keenan (guidance in EMG analysis), Marco Santello, Stephen Helms Tillery, Jonathan D. Posner, and Qiushi Fu (technical feedback), and Kevin Bair, Nicholas Fette, and Ryan Manis (data collection/processing). This material is based upon work supported by the National Science Foundation under Grant No. 0954254. Any opinions, findings, and conclusions or recommendations expressed in this material are those of the author(s) and do not necessarily reflect the views of the National Science Foundation.

References

Cole, K.J., Abbs, J.H., 1988. Grip force adjustments evoked by load force perturbations of a grasped object. Journal of Neurophysiology 60, 1513–1522.
Cole, K.J., Johansson, R.S., 1993. Friction at the digit–object interface scales the sensorimotor transformation for grip responses to pulling loads. Experimental Brain Research 95, 523–532.
De Gregorio, M., Santos, V.J., 2010. Rotational object perturbations result in characteristic types of kinematic grip responses. In: Proceedings of the Annual Meeting of the American Society of Biomechanics. Providence, RI.
Di Fabio, R.P., 1987. Reliability of computerized surface electromyography for determining the onset of muscle activity. Physical Therapy 67, 43–48.
Edin, B.B., Westling, G., Johansson, R.S., 1992. Independent control of human finger-tip forces at individual digits during precision lifting. Journal of Physiology (Lond) 450, 547–564.
Goodwin, A.W., Jenmalm, P., Johansson, R.S., 1998. Control of grip force when tilting objects: effect of curvature of grasped surfaces and applied tangential torque. Journal of Neuroscience 18, 10724–10734.
Häger-Ross, C., Cole, K.J., Johansson, R.S., 1996. Grip-force responses to unanticipated object loading: load direction reveals body- and gravity-referenced intrinsic task variables. Experimental Brain Research 110, 142–150.
Häger-Ross, C., Johansson, R.S., 1996. Nondigital afferent input in reactive control of fingertip forces during precision grip. Experimental Brain Research 110, 131–141.
Hodges, P.W., Bui, B.H., 1996. A comparison of computer-based methods for the determination of onset of muscle contraction using electromyography. Electroencephalography and Clinical Neurophysiology 101, 511–519.
Jenmalm, P., Dahlstedt, S., Johansson, R.S., 2000. Visual and tactile information about object-curvature control fingertip forces and grasp kinematics in human dexterous manipulation. Journal of Neurophysiology 84, 2984–2997.
Johansson, R.S., Häger, C., Bäckström, L., 1992a. Somatosensory control of precision grip during unpredictable pulling loads. III. Impairments during digital anesthesia. Experimental Brain Research 89, 204.
Johansson, R.S., Häger, C., Riso, R., 1992b. Somatosensory control of precision grip during unpredictable pulling loads. II. Changes in load force rate. Experimental Brain Research 89, 192–203.
Johansson, R.S., Riso, R., Häger, C., Bäckström, L., 1992c. Somatosensory control of precision grip during unpredictable pulling loads. I. Changes in load force amplitude. Experimental Brain Research 89, 181–191.
Johansson, R.S., Westling, G., 1987. Signals in tactile afferents from the fingers eliciting adaptive motor responses during precision grip. Experimental Brain Research 66, 141–154.
Johansson, R.S., Westling, G., 1988. Programmed and triggered actions to rapid load changes during precision grip. Experimental Brain Research 71, 72–86.
Jones, L.A., Hunter, I.W., 1992. Changes in pinch force with bidirectional load forces. Journal of Motor Behavior 24, 157–164.
Jordan, K., Newell, K., 2004. Task goal and grip force dynamics. Experimental Brain Research 156, 451–457.
Kinoshita, H., Bäckström, L., Flanagan, J.R., Johansson, R.S., 1997. Tangential torque effects on the control of grip forces when holding objects with a precision grip. Journal of Neurophysiology 78, 1619–1630.
Kuo, P.H., Deshpande, A.D., 2010. Contribution of passive properties of muscle–tendon units to the metacarpophalangeal joint torque of the index finger. In: Proceedings of the 3rd IEEE RAS and EMBS International Conference on Biomedical Robotics and Biomechatronics, pp. 288–294.
Pawluk, D.T., Howe, R.D., 1999. Dynamic lumped element response of the human fingerpad. Journal of Biomechanical Engineering 121, 178–183.
Wing A.M., Flanagan J.R., 1998. Anticipating dynamic loads in handling objects. In: Proceedings of the ASME Dynamic Systems and Control Division, pp. 139–143.